



## **AIAA 10-8134**

### **Electrostatic Inflation of Membrane Space Structures**

Laura A. Stiles, Hanspeter Schaub, Kurt K. Maute

*University of Colorado, Boulder, CO 80309-0431*

Daniel F. Moorer, Jr.

*Wacari Group, Boulder, CO 80302*

**AAS/AIAA Astrodynamics Specialists Conference**  
**August 2–5, 2010 / Toronto, ON**

# Electrostatic Inflation of Membrane Space Structures

Laura A. Stiles\*, Hanspeter Schaub†, Kurt K. Maute‡  
*University of Colorado, Boulder, CO 80309-0431*

Daniel F. Moorer, Jr.§  
*Wacari Group, Boulder, CO 80302*

**This paper presents a novel lightweight and compactly storable space structure concept where electrostatic forces are used to inflate a lightweight membrane structure. This gossamer structure is given an absolute electrostatic charge through active charge emission, leading to repulsive electrostatic forces which inflate the loose membranes into a semi-rigid structure. The electrostatic forces required in GEO and LEO orbits to maintain shape and offset disturbing orbital forces, such as differential gravity, differential solar radiation pressure and drag, are investigated. Challenges to the implementation of this concept include the plasma Debye shielding, complex structural dynamics, and the time varying space plasma environment. Successful terrestrial laboratory experiments of electrostatically inflating simple prototype gossamer structures are discussed. While the structure must compensate for a strong 1-g differential gravity in the lab, these experiments demonstrate feasibility of this concept as space applications would need to contend with much small differential perturbations.**

## I. Introduction

Gossamer spacecraft have been the subject of space hardware research for many decades. These lightweight, thin structures provide an alternative to the traditional mechanical systems which are typically more expensive, massive, and complex. Many different applications of gossamer space hardware have previously been explored, and a select few have been successfully employed in space. Examples of early work in inflatable structures include the development of the mylar ECHO balloons in 1958 at NASA. The ECHO I sphere, which was launched in 1960, successfully served as a communications reflector in space for several months.<sup>1</sup> L'Garde Inc. made many early contributions to the field of deployable technology, including the support for NASA to the launch an inflatable antenna from the Space Shuttle.<sup>2</sup> Examples of present day gossamer spacecraft research include solar sail technology,<sup>3</sup> inflatable solar arrays,<sup>4</sup> and space habitats.<sup>5</sup>

Common methods for actuation of gossamer structures include inflation via pressurized gas, sublimating chemicals, or evaporating liquids.<sup>6</sup> This paper explores a novel method for inflation of space structures by controlling the absolute electrostatic charge. Electrostatic charging has often been considered more of a challenge than an opportunity for space structures due to damage to spacecraft components caused by electrostatic discharge among differentially charged components. The presented concept, however, would make use of absolute spacecraft charging to self-repel structural members for deployment and to increase structural stiffness. The concept of electrostatic inflation is illustrated in Figure 1.

---

\*Graduate Research Assistant, Aerospace Engineering Sciences Department, University of Colorado, Boulder, CO. AIAA student member, AAS student member

†Associate Professor, H. Joseph Smead Fellow, Aerospace Engineering Sciences Department, University of Colorado, Boulder, CO. AIAA Associate Fellow, AAS member

‡Associate Professor, H. Joseph Smead Fellow, Aerospace Engineering Sciences Department, University of Colorado, Boulder, CO

§President, Wacari Group LLC, Boulder, CO

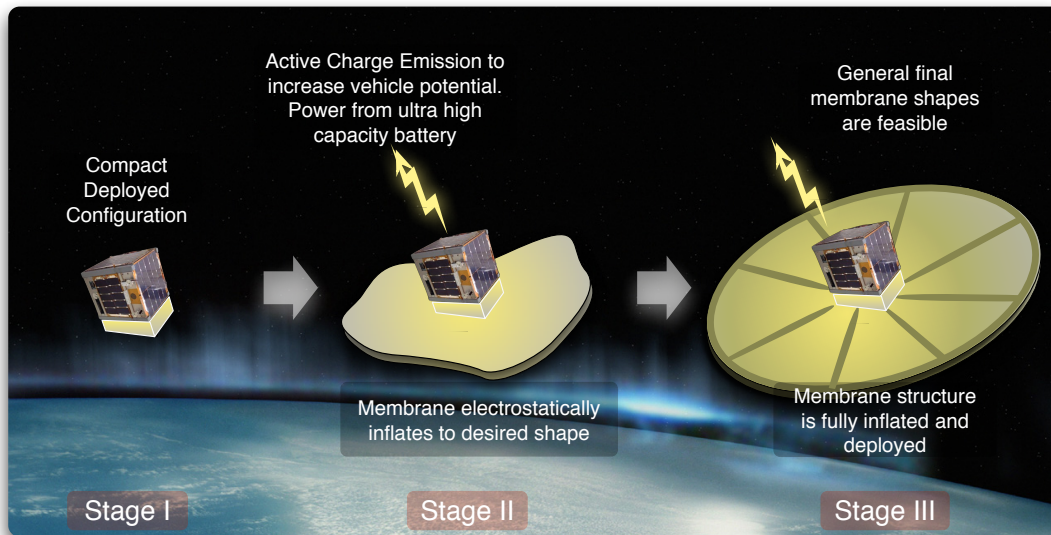


**Figure 1: Electrostatic inflation concept**

The concept of electrostatics for control of space structures has been studied for many decades. The previous research has mainly focused on using electrostatics to precisely control the shape of membrane surfaces whose outer edges are held in place by a solid structure. A US patent by J.H. Cover filed in 1966 describes an invention for using electrostatics to control the surface of a reflector dish in space.<sup>7</sup> This patent also discusses how electrostatic forces can be created using active charge emission using only Watt levels of power at geosynchronous orbit altitudes. However, the electrostatics are only used to shape a single membrane structure. In contrast, the concept presented in this paper uses electrostatics to inflate a self-supporting layered membrane structure. Electrostatically controlling the surface of membrane mirrors in space has also been studied, an example of such is the work of Errico, et. al. in Reference 8. These designs significantly differ from the proposed membrane structure inflation as the mirror and reflector technology requires an external ring structure to support the surfaces. With inflation of the membrane structures, the gossamer structure is completely and compactly stowed until the charge level is increased to cause the entire structure to inflate.

Another field of related research is Coulomb control for proximity flying spacecraft. This application aims to raise the absolute potential of the spacecraft to control the electrostatic interactions with surrounding craft. Actively charging a craft to a few kilovolts causes electrostatic forces between the craft of micro- to milli-Newton levels with millisecond charging time.<sup>9,10</sup> In References 11 and 12 the Coulomb force is explored to develop static virtual structures subject both to the gravitational and electrostatic force fields. Feedback control strategies of such virtual structures have only been developed for simple 2- and 3-craft systems thus far.<sup>13,14</sup> A related concept to the proposed electrostatic membrane structure is the Tethered Coulomb Structure (TCS) proposed in Reference 15. Here the complex charged relative orbital motion is constrained through the use of very thin tethers interconnecting the charged nodes. The electrostatic force is used to create an inflationary pressure to ensure positive tether tension at all times. Thus, the TCS can essentially be considered as a larger scale, discrete element version of an electrostatically inflated space structure. In contrast to the TCS, the differential orbital perturbations that drive charging requirements will be very different due to the larger mass of the TCS system (50-100 kg nodes), versus the sub-kilogram membrane structure.

The challenge of controlling the potential of a body in space has been flight tested with successful results. The SCATHA (Spacecraft Charging at High Altitudes) experiment was one of the spaceflight experiments which demonstrated use of ion and electron guns to control spacecraft surface potential to 10-20 kV.<sup>16,17</sup> Even without active charging, spacecraft can charge up to many kilovolts in the plasma environment. The highest recorded natural charging event occurred on the ATS-6 spacecraft, reaching a potential of -19 kV during an eclipse period of the GEO orbit.<sup>18</sup> While the previous two examples are space missions with active charge control at geosynchronous altitudes, the following mission is an example of a charging experiment at Low Earth Orbit (LEO). The SPEAR I mission employed active charging of test spheres in LEO with an altitude of approximately 350 km.<sup>19</sup> Using a capacitor, a positive potential of 45.3 kV was applied to two 10 cm radius spheres attached to a rocket body.<sup>19</sup> The current CLUSTER mission

also employs active charge control through continuous charge emission to servo the spacecraft absolute potential to a desired near-zero charge level.

The charge control of a spacecraft is, however, complicated by the presence of the plasma environment. While at geostationary altitudes the charge control can be achieved with low electrical power levels,<sup>20</sup> the relatively cold and dense plasma at low Earth orbits makes charge control more challenging. LEO applications would require more power, and the electrostatic field about a charged body is more quickly negated by the surrounding plasma charge.

The purpose of this paper is to present the concept of electrostatic inflation for space structures. A first-order investigation is performed to determine required charge densities for simple electrostatically inflated structures to maintain a desired nominal shape after deployment. The potentials must be high enough to produce sufficiently large electrostatic forces for self-repulsion to negate the differential forces from gravity, solar radiation pressure, and/or atmospheric drag that would be experienced in orbit.

As the space environment varies greatly with altitude, this paper also addresses the regions of applicability for electrostatic inflation. Current research shows that plasma temperatures and densities at GEO make the use of electrostatics for inflation very feasible, yet LEO altitudes pose a more challenging space plasma environment that must be considered for these applications. Lastly, this paper describes the results of lab experiments which investigate if the electrostatic inflation concept is experimentally verifiable, even in the 1-g environment of Earth's surface. Any future modeling of the complex charge membrane dynamics and deployment control will require validation and verification. Having repeatable Earth-based experiments will enable the mathematical modeling of the associated physics to be tested, as well as new material and shape concepts to be tested.

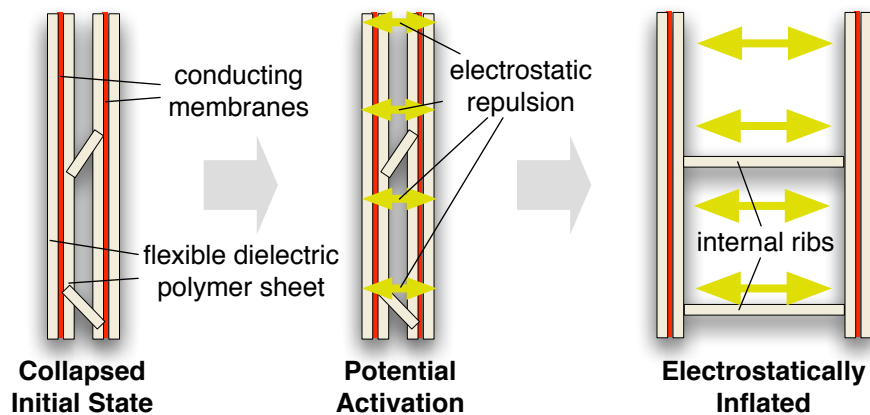
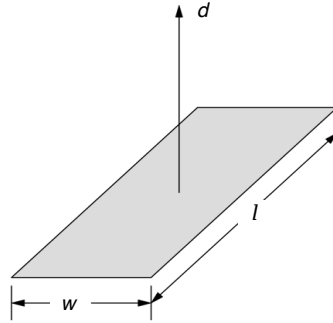


Figure 2: Sample open-ended membrane rib structure undergoing electrostatic inflation

## II. Electrostatic Inflation Concept

The concept of electrostatic inflation is applicable for gossamer structures on spacecraft. With no outside force for inflating the structure, there is no rigidity or stiffness for maintaining a nominal desired shape or configuration. Applying electric charge to a sandwiched or layered gossamer structure provides an inflation pressure due to repulsive electrostatic forces between the charged layers, per Coulomb's law. Elements of the structure can self-repel with this applied potential, thus inflating to a semi-rigid structure, much like inflation of an airbag with gas. However, in contrast to gas-inflated structures, the electrostatically inflated structure does not suffer from sensitivities to membrane punctures. In fact, the simple concepts considered in this paper are open ended membrane structures resembling more the ribbed open structure of a ram-air parachute than that of a fully enclosed balloon.

The electrostatic inflation concept is particularly applicable to structures such as arrays, solar power reflectors, or drag augmentation devices for de-orbiting and space debris avoidance purposes. In applying electrostatics for inflation of these and other space apertures, there is the potential to significantly decrease mass, while reducing the associated deployment oriented power and packing volume for deployable structures. A large ratio of deployed volume to stowed volume is very advantageous, especially in highly volume-constrained spacecraft such as CubeSats. Many apertures have performance directly related to their deployed surface area while their design is limited by available pre-launch stowed volume.



**Figure 3: Definitions for rectangular plate field model**

The study of the required charge densities for inflated structures in this paper is considering a simple 2-plate sandwich structure with ribs, such as the one shown in Figure 2. The ribs are assumed to only be able to provide tensile forces between the two outer ribs. If compressive forces are applied, then the ribs are modeled to buckle immediately and no longer interact with the outer membranes. The membranes themselves are analytically modeled as flat plates. Depending on the membrane material stiffness, such a sandwich structure would cause small amounts of pillowing between the ribs. Such effects are not considered in this first order study. Rather, this paper investigates what surface charge densities are required on the plates such that a sufficient electrostatic repulsion is achieved to overcome differential orbital perturbations. Future work will investigate higher order modeling of the complex membrane shape interactions with the disturbance forces, rib segments, space environment and the dominant electrostatic force fields.

The electrostatic field due to a finite rectangular plate of the sandwich structure is:<sup>21</sup>

$$E = \frac{4\sigma}{4\pi\epsilon_0} \arctan \left( \frac{lw}{4d\sqrt{\left(\frac{l}{2}\right)^2 + \left(\frac{w}{2}\right)^2 + d^2}} \right) \quad (1)$$

Here  $\sigma$  is the surface charge density, while the plate dimensions  $w$ ,  $l$  and  $d$  are illustrated in Figure 3. Note that the electrostatic field strength  $E$  in Eq. (1) is only valid moving along the rectangular plate center axis shown in Figure 3. The actual fields are complicated by issues such as edge effects. However, this simplified analytical model is sufficient for the purpose of this paper as it captures the dominant electrostatic field of the plate if  $w$  and  $l$  are large in comparison to the membrane structure thickness  $d$ . For the proposed Gossamer structures with square meters of surface areas, the membrane layer separation distance  $d$  is considered to be on the order of centimeters. To fully understand the actual fields, numerical simulation is required.

There are many challenges for electrostatic inflation that are beyond the scope of this concept paper. One challenging issue is the storage and deployment of the structure. In laboratory experiments to inflate a structure such the one illustrated in Figure 2, a non-conducting gap or layer between conducting surfaces is required for electrostatic inflation to occur. Without a gap, the layers of charged conducting sheets do not separate. For electrostatic inflation, it is speculated that non-conducting segments are needed between the conducting surfaces such as gaps or un-polarized dielectric layers. Understanding the physical mechanism between sticking layers remains as future work. In lab experiments, a small gap with air between surfaces has shown sufficient for inflation to occur. These results are discussed in the last section. The following work assumes that the two plates are already minimally separated such that electrostatic repulsion can occur. Of interest is the following: how does the electrostatic repulsion between the plates vary with the separation distance, and what charge densities  $\sigma$  are required to be able to overcome the differential orbital perturbations experienced either at GEO or LEO altitudes.

### III. Space Weather Impact

#### A. Debye Shielding of Point Charges

In the plasma environment of space, electrons and ions rearrange in the presence of a disturbing electric field to maintain macroscopic neutrality.<sup>23</sup> This phenomena, known as Debye shielding, will effectively shield the electrostatic field of a charged object in a plasma, such as an electrostatically inflated structure. To determine the potential near a charged object in a plasma, the number density of charged particles must be known. An expression for the electron

density and ion density are given in Eqs. (2),<sup>23</sup> where  $k$  is the Boltzmann constant,  $T$  is temperature,  $\phi$  is the potential due to a charge, and  $n_0$  is a constant particle density where  $n_e(\infty) = n_i(\infty) = n_0$ .

$$n_e = n_0 e^{\frac{e\phi}{kT_e}} \quad (2a)$$

$$n_i = n_0 e^{-\frac{e\phi}{kT_i}} \quad (2b)$$

Using these definitions for particle number densities, Poisson's equation is written as:

$$\nabla^2 \phi = -\frac{\rho}{\epsilon_0} = \frac{n_0 e}{\epsilon_0} \left( e^{-\frac{e\phi}{kT}} - e^{\frac{e\phi}{kT}} \right) \quad (3)$$

This classical development continues under the assumption that potential energy of the field is much smaller than the kinetic energy of the particles, or ( $e\phi \ll kT$ ). With this assumption the simplified expression is yielded:

$$\nabla^2 \phi = \frac{2}{\lambda_D} \phi \quad (4)$$

where the parameter,  $\lambda_D$  is a parameter known as the Debye Length. The Debye length describes the distance at which a charge is essentially shielded by the plasma if ( $e\phi \ll kT$ ) is true. The Debye length is determined by plasma conditions through:

$$\lambda_D = \left( \frac{\epsilon_0 kT}{n_e e^2} \right)^{\frac{1}{2}} \quad (5)$$

where  $e$  is the elementary charge. This particular form of the Debye length computation assumes that the negative plasma electrons dominate the electrostatic charge shielding. The simplified form of Poisson's equation has a well known analytical solution for the potential surrounding a point charge,  $q_1$ , (or a charged sphere with total charge  $q_1$ ) in spherical coordinates given by:

$$\phi = \frac{k_c q}{r} e^{-\frac{r}{\lambda_D}} \quad (6)$$

The Debye shielded electrostatic force experiences by a 2nd point charge  $q_2$  is derived using Equation (6):

$$F = \nabla \phi \cdot q = \frac{k_c q_1 q_2}{r^2} e^{-\frac{r}{\lambda_D}} \left[ 1 + \frac{r}{\lambda_D} \right] \quad (7)$$

While this force computation is only valid for point charges, and not the plate models considered in this paper, Eq. (7) provides insight into how the plasma Debye length can limit the electrostatic actuation. Equation (7) allows for quick analytical computation of the electrostatic force for a point charge or spherical assumption, as no simple analytical expression describes the electrostatic force between two plates. Numerical analysis is quickly required as geometry becomes more complicated. The following discussions consider conditions under which the Debye shielding can be treated as negligible in regard to the electrostatic force computation. This can be achieved through either flying the electrostatically inflated membrane structures at particular orbit altitudes, or employing large potentials.

## B. Orbit Regions Applicable for Electrostatic Inflation

Debye shielding effects the feasibility of using electrostatics in a plasma environment. In the Low Earth Orbit region, Debye lengths are typically on the order of milli- or centimeters, depending on the orbit altitude. Table 1 shows the extremes of Debye lengths experienced in LEO at an orbit altitude of approximately 350 m, as predicted by the International Reference Ionosphere model and reported in Reference 24.

In earlier work on Coulomb control of free-flying charged spacecraft, or the electrostatic inflation of TCS concepts over several meters, this aggressive Debye shielding prevented such concepts from being considered at LEO.<sup>10,15</sup> However, with the electrostatically inflated membrane structures, even with surface areas of multiple square meters, the electrostatic force only has to occur across the membrane gap layer separation distance  $d$  which can be on the order of centimeters. If the separation distance between the plates of a sandwich structure in LEO is greater than a few millimeters or centimeters, or of the order of the local Debye length, then the plates would not experience a significant electrostatic force and the inflation concept would not be feasible. This argument assumes that the membrane potential

$\phi$  satisfies the condition that ( $e\phi \ll kT$ ). Thus, if small membrane gaps  $d$  less than of a centimeter are assumed, then even with the aggressive Debye shielding assumptions the electrostatic inflation could still occur at LEO. With the proposed concept it is not necessary for the electrostatic repulsion to occur between a membrane segment and the entire opposing membrane plate. Rather, the membrane structure provides some geometric stiffening through the tensioning membrane itself. Compared to earlier work on free-flying charged spacecraft where the formation size is directly limited by the electrostatic force drop off with separation distance, the membrane structure can scale to comparatively large dimensions as the electrostatic force does not need to act along the plate  $w$  and  $l$  dimension, only across the much smaller  $d$ .

In the GEO regime, the Debye length is generally on the order of hundreds of meters. However, these values can vary drastically with the solar storm activities heating up part of the plasma sheath, or pushing the lower and colder plasma pause conditions into the GEO altitudes.<sup>25</sup> The upper and lower bounds of possible geostationary Debye length values are shown in Table 1, as well as the nominal value. These Debye lengths are based on observations from the ATS-5 and ATS-6 spacecraft given in References 26 and 27. The small separation distances between proposed membrane plate structures compared to the comparatively large Debye lengths yield nearly negligible effects from the shielding, and the field decreases proportional to the  $1/r^2$  vacuum electrostatic field dropoff. This is true even for the very worst GEO plasma weather conditions being considered.

**Table 1: Range of Feasible Plasma Debye Lengths**

	Smallest Debye Length	Nominal Debye Length	Largest Debye Length
LEO Environment	0.002 m	0.005 m	0.013 m
GEO Environment	4 m	200 m	743 m

### C. High Potentials with Reduced Charge Shielding

In the development of the analytical Debye shielded electrostatic potential in Eq. (??) about a point charge, there is an assumption that  $e\phi/kT \ll 1$ . Considering a spacecraft at GEO, the plasma conditions at this altitudes satisfy this requirement if the applied potential is low. As the potential becomes large, however, this assumption begins to be violated. Assuming an average GEO plasma particle temperature of 10 eV,<sup>9</sup> the critical ratio  $e\phi/kT$  becomes larger than 1 for a potential of approximately 10 kV. As discussed earlier, natural charging of spacecraft can reach potential levels greater than 10 kV, with recorded events up to -19 kV.<sup>18</sup> At LEO altitudes, even a small spacecraft potential violates the assumption, as the temperature in LEO is much lower than GEO. Assuming an average particle temperature of 1 eV,<sup>9</sup>  $e\phi/kT$  becomes larger than 1 for a potential of approximately 1 V. Thus, of interest is how these neglected higher order terms of  $e\phi/kT$  in Poisson's equations impact the actual electrostatic force experienced between two bodies.

Because the proposed concept considers potentials of the order of multiple kilo-volts, the assumption that  $e\phi/kT \ll 1$  is quickly violated in both LEO and GEO. When spacecraft reach high potentials, a numerical solution is necessary to determine a better estimate of the potential around an electrostatically charged object. The numerical solution is reached by satisfying Poisson's equation and the Vlasov equation of motion for particles, as fully described in Reference 28.

By solving the full Poisson-Vlasov partial differential equations, it is assumed that the plasma is collisionless, particle densities are single-Maxwellian, and the effects of ramming ions experienced at LEO due to the large spacecraft orbital velocity are ignored. Results from a numerical simulation of potentials surrounding a sphere at a potential of 30 kV in a cold GEO plasma are shown in Figure 4. The Debye shielded force from Equation (7) represents the lower bound for the achievable electrostatic force, while the vacuum electrostatic force computation represents the upper limit. Note that the actual electrostatic force between two charged particles lies between the vacuum force model and the conservative partially shielded model in Eq. (7). This reduction of the Debye shielding influence is discussed by Murdock et. al for the electrostatic asteroid tug application in Reference 29 The effective Debye length is the distance over which the electrostatic force reduction is equivalent to that of the simplified force model in Eq. (7). From the simulation of the electrostatic potential due to a 30 kV sphere, the effective Debye length is approximately 3.5 times larger than the predicted Debye length. The distance for the plasma to shield a charge is therefore 3.5 times farther, thus allowing for greater separation distances between plates. Murdock et. al. discuss how the effective Debye lengths for the asteroid application can be 100 times larger than the regular Debye length. In the numerical GEO force comparison in Figure 4 the effective Debye lengths are on the order of three times larger. As a result, as the membrane potentials are

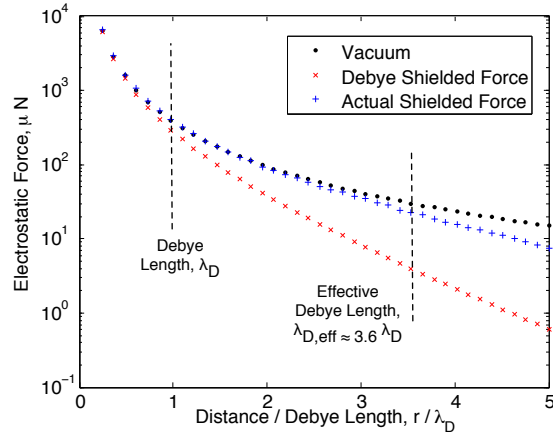


**Figure 4: Comparison of analytical and numerical predictions of electrostatic force experienced in a cold plasma at GEO due to a 0.5 m radius sphere,  $\phi = 30kV$ ,  $\lambda_D = 4.1m$**

large relative to the plasma, a condition which is quickly true for LEO applications, the resulting electrostatic shielding is significantly reduced, and the electrostatic forces are closely modeled by the vacuum electrostatic expression. Thus, electrostatic inflation at LEO over membrane separation distances of a fraction of a meter are feasible.

In this section, the required electrostatic forces and charge densities to maintain inflation of a 2-plate sandwich structure in GEO and LEO are calculated for different orbit configurations: orbit radial, along-track, and orbit normal. Figure 7 illustrates these three possible configurations. The disturbance forces considered for the inflated membrane structure are solar radiation pressure, differential gravity, and atmospheric drag. The dominating perturbation varies depending on the the orientation and orbit region.

## IV. Orbit Perturbations Affecting Electrostatic Inflation

### A. GEO Orbit Perturbations

For electrostatic inflation, potentials must be high enough to produce sufficient electrostatic forces for self-repulsion to negate the differential forces from gravity, solar radiation pressure, and drag that would be experienced in orbit. These perturbations are all distributed over the surface of the structure. In the GEO environment atmospheric drag is not a consideration. The effect of differential gravity depends on the orbit configuration as this perturbation will tension the structure in the radial configuration, compress the structure in the normal configuration, and have no effect in the along-track configuration.

The linearized differential gravity in the orbit radial configuration shown in Figure 5(a) is given by Equation (8) where  $\mu$  is the gravitation parameter,  $r_c$  is the radius from Earth, and  $d$  is the separation distance of the membrane plates.<sup>15</sup> In this configuration the differential gravity force will aid in tensioning the structure, as the plate nearest to

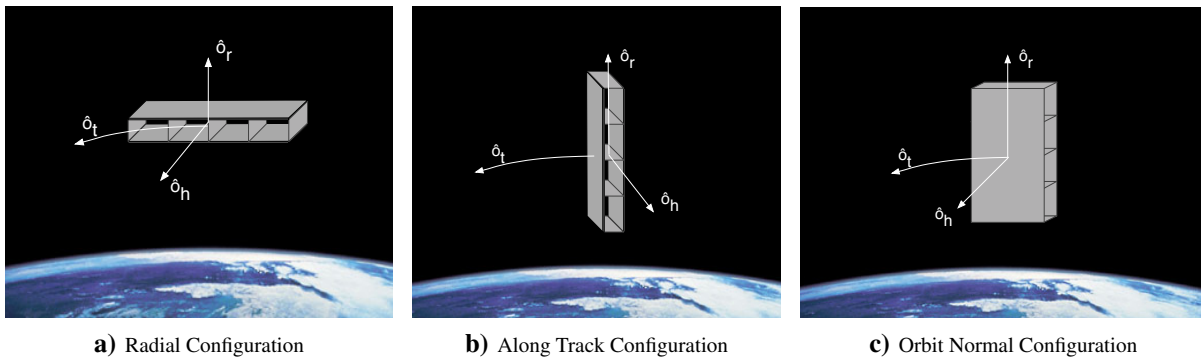


**Figure 5: Possible orbital configurations of the sandwich structure**

Earth will experience a stronger force due to gravity.

$$\delta F_{g,\text{radial}} \approx m \frac{3\mu}{r_c^3} d \quad (8)$$

For this study, mass is estimated from density,  $\rho$  and approximate material volume with area,  $A$ , and thickness,  $t$ :

$$m = \rho A t \quad (9)$$

75 gauge Aluminum coated Mylar, a possible material to be used for the proposed gossamer space structure, is used as the baseline material for this study. Thickness and density of this material are 19 microns and  $1.40 \text{ g/cm}^3$ , respectively. The mass contribution of the ribs is neglected here. To eliminate area dependence in the calculations, the differential pressure is calculated as follows:

$$\delta P_{g,\text{radial}} = \frac{\delta F_{g,\text{radial}}}{A} \approx \rho t \frac{3\mu}{r_c^3} d \quad (10)$$

For the along-track configuration shown in Figure 5(b) the differential gravity force and pressure are essentially zero:

$$\delta F_{g,\text{along-track}} \approx \delta P_{g,\text{along-track}} \approx 0 \quad (11)$$

In the orbit normal configuration in Figure 5(c), differential gravity will tend to compress the structure. The linearized differential gravity force in this configuration is given by Eq. (12).<sup>15</sup>

$$\delta F_{g,\text{normal}} \approx -m \frac{\mu}{r_c^3} d \quad (12)$$

Similarly, the differential gravity pressure is:

$$\delta P_{g,\text{normal}} = \frac{\delta F_{g,\text{normal}}}{A} \approx -\rho t \frac{\mu}{r_c^3} d \quad (13)$$

These differential gravity forces, however, are very small in comparison with the solar radiation pressure. This result differs from the perturbation analysis for Coulomb formation flying or tethered Coulomb structures in which the differential gravity has a much larger effect. The cause for this difference is that both separation distances and masses are orders of magnitude smaller for the gossamer 2-plate rib structure.

The equation for the disturbance force from solar radiation pressure is given by:<sup>30</sup>

$$P_{SRP} = \frac{F_{SRP}}{A} = p_{SR} c_R \quad (14)$$

where  $p_{SR} = 4.57e^{-6} \frac{N}{m^2}$  is the nominal solar pressure at 1 AU from the sun,  $c_R$  is the reflectivity, and  $A$  is the area exposed to the sun. Note that the solar radiation pressure is independent of separation distance, area and orbit altitude. This pressure will therefore be identical at LEO and GEO orbits.

These GEO perturbations force magnitudes are next compared for the three configurations illustrated in Figure 7:

### 1. GEO Orbit Radial Configuration

The orbit radial configuration is defined as the large areas of each plate to be nadir facing, as shown in Figure 7(a). Considering a worst case scenario, the solar radiation pressure would act directly normal to one plate, as shown in the force diagram in Figure 6. To avoid compression of the membrane structure, the inflationary electrostatic force must be greater than this differential solar radiation force. Figure 7(a) shows a comparison of the magnitudes of disturbing pressures experienced at GEO for the sandwich structure. Considering the disturbance pressures versus using the forces has the benefits that the disturbances per unit area can be considered. Thus, the following results are independent of the membrane structure area  $A$ . Note that the differential solar pressure dominates over the differential gravity even with large 1 meter separation distances. This is in strong contrast to the research results on free-flying charged spacecraft where differential gravity terms dominate. With the membrane structures the area to mass ratio is significantly larger, allowing the solar radiation pressure to be orders of magnitude larger. As a result the tensioning ability of the radial differential gravity term provides negligible relief on the overall inflationary force requirement.

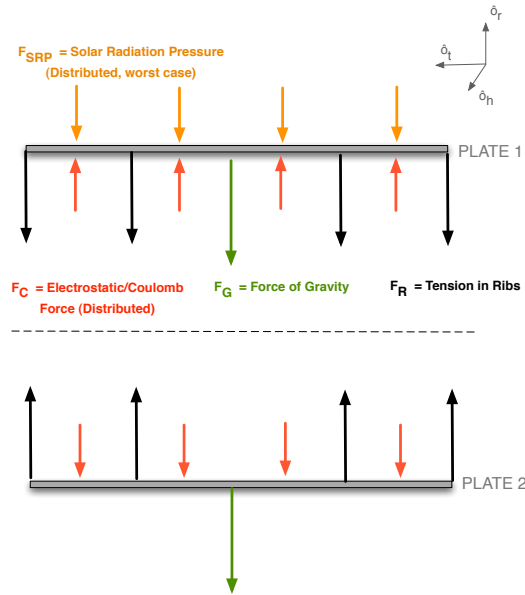


**Figure 6: Forces on the structure in the radial configuration**

2. *GEO Along-Track Configuration*

In the along-track configuration, differential gravity has no effect on the sandwich structure. The only disturbance force is therefore solar radiation pressure, and the separation distance of the plates will have no effect on the required electrostatic force for inflation. Again assuming a worst case alignment of the incident sun light with respect to the outer membrane surface, the resulting compressive solar radiation pressures are shown in Figure 7(b). Because this differential solar radiation pressure model is independent of the membrane separation distance, the minimum required inflationary force is a fixed value regardless of the sandwich structure thickness.

3. *GEO Orbit Normal Configuration*

Figure 7(c) shows a comparison of the magnitudes of disturbing pressures experienced at GEO for an inflated sandwich structure in the orbit normal configuration. These magnitudes are nearly identical to the radial configuration, with the exception that in the normal configuration, differential gravity tends to compress the structure instead of providing tension, as in the radial configuration. Again the solar pressure dominates the required inflationary force for this GEO configuration.

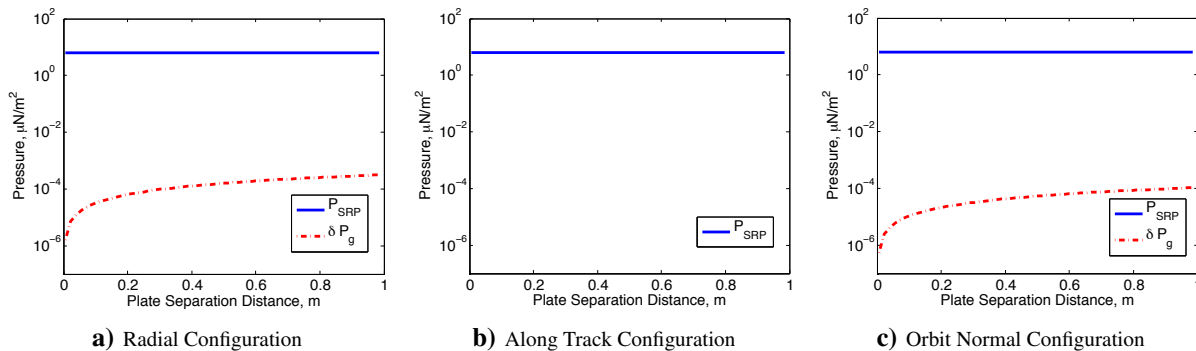


**Figure 7: Magnitudes of disturbance pressures in the radial, along-track, and normal configurations at GEO, mass  $m = 0.01kg$**

## B. Perturbations in LEO

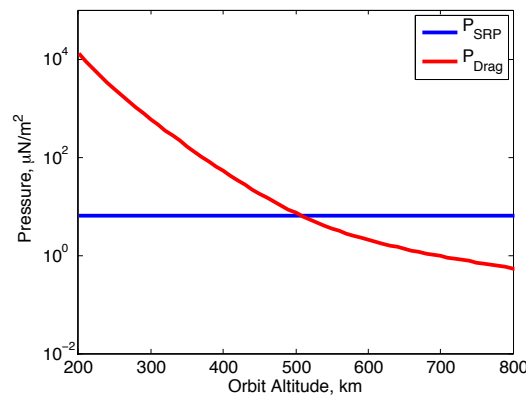
Next, let us consider a membrane structure which is flying at LEO altitudes. In addition to the differential gravity pressures and solar radiation pressure expressed in Equations (10), (13), and (14), the perturbation from atmospheric drag is also considered. The drag force at these altitudes cannot be neglected as a perturbation as it may be at GEO altitudes. The force on the leading plate is calculated with:<sup>30</sup>

$$F_D = -\frac{1}{2}C_D A \rho v_{rel}^2 \frac{\mathbf{v}_{rel}}{|\mathbf{v}_{rel}|} \quad (15)$$

Again, to eliminate area dependence, the differential pressure from drag is calculated with:

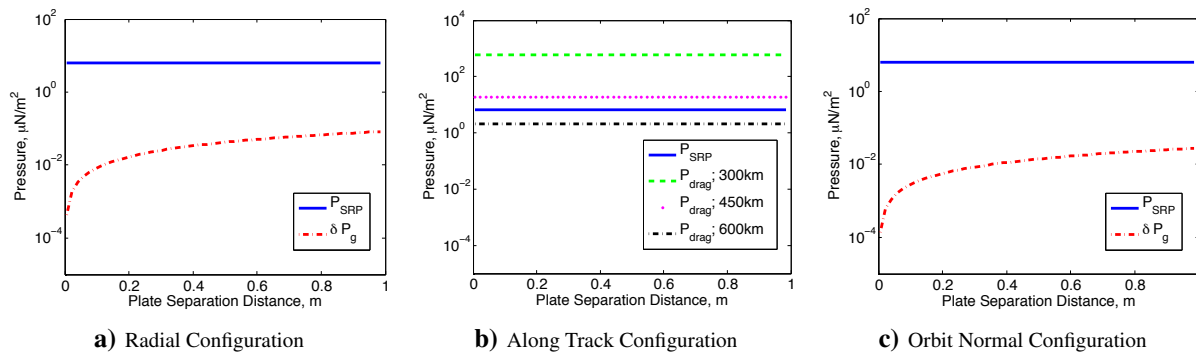
$$P_D = -\frac{1}{2}C_D \rho v_{rel}^2 \frac{\mathbf{v}_{rel}}{|\mathbf{v}_{rel}|} \quad (16)$$

This force, however, is only considered for the along-track configuration. Here the large area of one plate is bombarded by the rarified atmospheric particles, while the other plate is protected in the wake of the leading plate. The resulting differential drag force on the leading plate tends to compress the structure. In the orbit radial and normal configurations the differential drag forces are negligible as no significant area is presented relative to the incoming rarified atmosphere. For the sandwich structure with an area of 0.5 m<sup>2</sup> and a mass of 0.01 kg, a study is performed to determine the altitude at which the drag force diminishes versus the differential solar radiation forces. Values for atmospheric density are calculated using the MSIS-E-90 Atmospheric Model.



**Figure 8: Disturbance pressures as a function of altitude in LEO**

As shown in Figure 8, below approximately 500km the atmospheric drag pressure is the dominating perturbation. Above this altitude, the density becomes too low to have an appreciable effect. Below this altitude, the required charge densities to inflate a membrane structure must take the differential atmospheric draft into careful consideration.



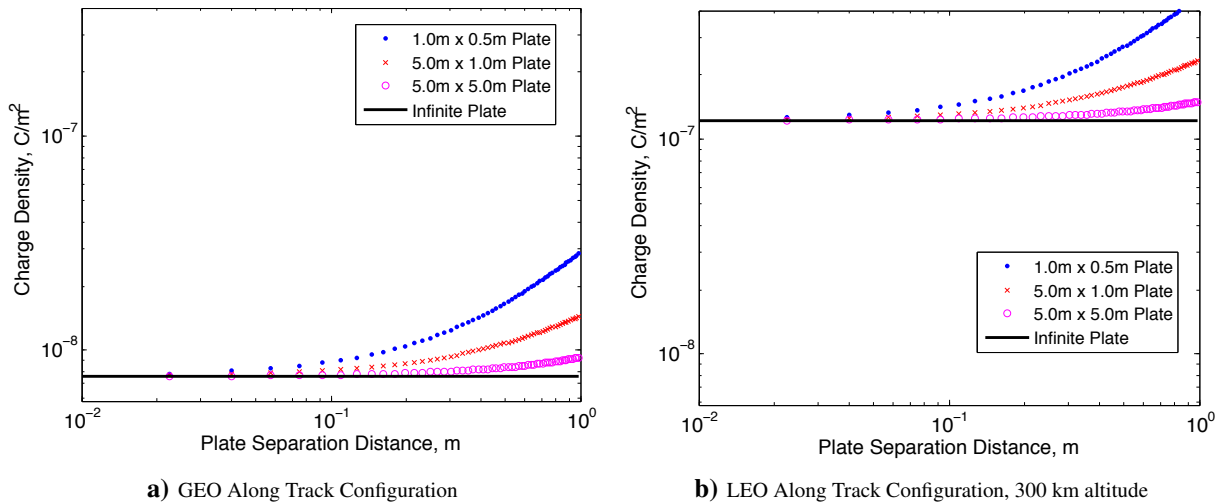
**Figure 9: Magnitudes of disturbance pressures in the radial, along-track, and normal configurations at LEO, mass  $m = 0.01kg$ , orbit altitude of 300 km with a range of altitudes shown for drag pressures**

Figure 9 displays the magnitudes of differential gravity, solar radiation and drag pressures at a LEO altitude of 300 km. The differential gravity pressure is approximately two orders of magnitude larger at this altitude than at GEO. The solar radiation pressure, however, is the same at LEO as GEO due to the independence from orbit altitude. For the along-track configuration pressures, shown in Figure 9(b), the drag pressure is displayed at three different orbit altitudes to demonstrate the dramatic effect of orbit altitude on drag in LEO. As was illustrated in Figure 8, below 500 km, the drag pressure dominates the solar radiation pressure. This is shown again in Figure 9(b), as the drag pressure at 450 km is larger than the solar radiation pressure, but at 600 km, the solar radiation pressure has become dominant. At 300 km, the drag pressure dominates by two orders of magnitudes. Therefore below 500 km, the drag force is clearly the perturbation that causes the largest effect and must be compensated for with sufficient electrostatic repulsion.

## V. Electrostatic Inflation

### A. Necessary Charge Densities

Electrostatic inflation of a structure occurs when an electrostatic potential is applied and the charges distributed on the surface repel each other, expanding the structure. As the structures are not simple shapes, such as a classical parallel plate capacitor, a relationship between the potential and charge is not analytically known. It is desired to analytically predict the required potential for inflation, but only the required charge density is understood at this time. Future work will investigate numerical electrostatic field modeling tools to determine the charge density to voltage relationship for the proposed sandwich membrane structures.



**Figure 10: Minimum required surface charge density for electrostatic Inflation at GEO and LEO for a range of plate areas**

To determine the required charge density, the force between the plates must first be understood. The electrostatic force  $F$  experienced by a charge  $q$  in an electric field  $E$  is given by Equation (17).

$$F = E \cdot q \quad (17)$$

The electrostatic force experienced by a charge above the center of a charged plate is therefore determined from Equations (1) and (17). When considering two plates, the force on the center of one plate due to the other is expressed assuming a constant surface charge density,  $\sigma$ , yielding a total charge of  $\sigma A$ . Assuming the charge density on each plate is equal, the force on each plate is determined as shown in Equation (18).

$$F = \frac{4\sigma^2 A}{4\pi\epsilon_0} \arctan \left( \frac{lw}{4d\sqrt{\left(\frac{l}{2}\right)^2 + \left(\frac{w}{2}\right)^2 + d^2}} \right) \quad (18)$$

This can be solved for the the required charge density  $\sigma$  to create a required inflationary pressure level ( $P_{req}$ ) which at

least matched the differential orbital pressure.

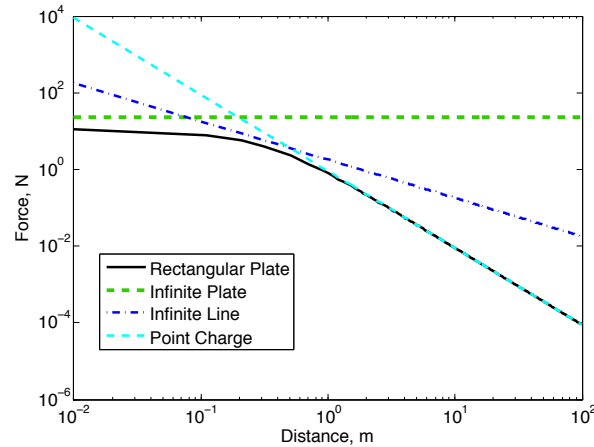
$$\sigma = \sqrt{\pi\epsilon_0 P_{\text{req}} / \arctan\left(\frac{lw}{4d\sqrt{\left(\frac{l}{2}\right)^2 + \left(\frac{w}{2}\right)^2 + d^2}}\right)} \quad (19)$$

Figure 10 shows the required charge densities to achieve inflation of sandwich structures, as calculated with Equation (19) for a range of plate areas in GEO and LEO. Also included in Figure 10 is the required charge density if the plates of the sandwich structure are modeled as infinite. Note that the infinite plate model results in a flat electrostatic field emanating from the plates, or equivalently a constant force. Thus, this simple model predicts a fixed membrane charge density for all plate separation distances considered. The smaller the plate separation  $d$  is, the closer these results approach the fixed charged density results of an infinite plate. However, square meter level plates having centimeter separations can yield appreciable changes in the charge density requirements from the infinite plate model.

The solar radiation pressure is considered the dominant GEO perturbation for which must be compensated, and drag is the dominant perturbation in LEO at the altitude of 300 km which was chosen for this simulation. The worst case required charge density for LEO (which occurs in the along-track configuration) is more than an order of magnitude larger than the worst case required charge density in GEO. The total charge on each plate of the sandwich structure remains below one microCoulomb in any orbit or configuration.

## B. Structural Stiffness

To understand the behavior of an electrostatically inflated structure, the compressive stiffness must be investigated. First, the electric field that will be experienced due to one plate of the sandwich structure is revisited. In the case of large plates at very small separation distances, the electric field behaves nearly as that of infinite plates. As the plates become smaller or the separation distances become large, the field is closely modeled by that of a point charge. Between these two extremes, the field can be modeled similarly to a line charge with a  $1/r$  dependence. These comparisons are shown in Figure 11 for a rectangular plate with an area of  $0.5 \text{ m}^2$ .



**Figure 11: Electrostatic force due to a rectangular plate,  $A = 0.5 \text{ m}^2$ ,  $\sigma = 20 \mu\text{C}/\text{m}^2$**

As the areas of the sandwiched membrane structure envisioned for applications of electrostatic inflation are very large compared to separation distances, making the weak assumption of infinite plates provides reasonable estimates of the fields and required charge densities. It must be noted that the electric field due to an infinite plate is not dependent on distance, as shown in Equation (20).

$$E_{\text{flat-plate}} = \frac{\sigma}{2\epsilon_0} \quad (20)$$

This independence from distance in the electric field and therefore the electrostatic force classically yields a compressional stiffness of zero in the system. In reality, the plates are not infinite, thus even though the dependence is small at close distances, there will still be some distance dependence and therefore a small amount of stiffness. Using the

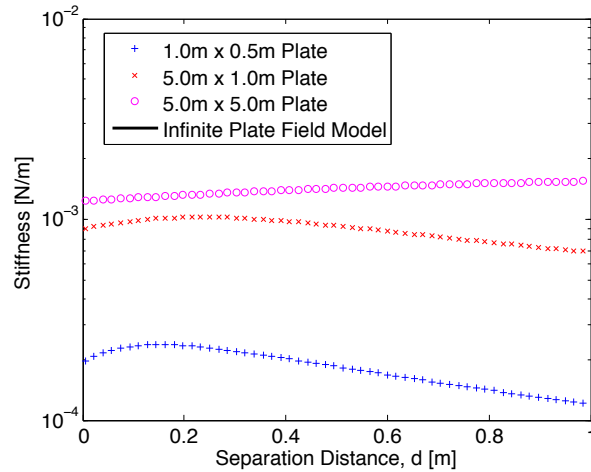


**Figure 12: Compressional stiffness of a sandwich structure for a range of areas; GEO orbit**

model of rectangular plates, the stiffness is found as shown:

$$k_s = \frac{\partial F}{\partial d} = \frac{4\sigma^2 A}{4\pi\epsilon_0} \frac{2lw(8d^2 + l^2 + w^2)}{(4d^2 + l^2)(4d^2 + w^2)\sqrt{4d^2 + l^2 + w^2}} \quad (21)$$

Figure 12 displays this stiffness relationship for a range of plate areas. These stiffness values were calculated using the required electrostatic pressure to offset orbit perturbations in the radial configuration at GEO. It is interesting to note that each curve has a maximum, suggesting an optimal separation distance for a particular plate size.

Regardless of the stiffness of the structure, the structure will remain inflated if the electrostatic force is larger than a distributed perturbation force. A dominating electrostatic force must be maintained to avoid a collapse in the structure. With this concept, however, a structure collapse would not be a failure. If the structure deformed temporarily, such as during a rotational maneuver of the spacecraft, the electrostatic charge would reinflate the structure to the desired form. Future work includes studying the rotational stiffness of a sandwich structure, as well as different rib configurations to optimize structural benefits.

## VI. Experimental Results

An experimental setup was designed to aid in testing and understanding the concept for electrostatic inflation. The setup consists of an aluminized Mylar ribbed sandwich structure resting on a conducting surface which is connected to a high voltage power source. Figure 13 shows the rib structure atop the conduction surface. In this 1-g test environment, the forces on the lower plate are always balanced by the normal force of the object upon which it rests. The other plate is subjected to the Coulomb force to inflate, the compressive force of gravity, and tension in the ribs to hold the structure together. This setup is much like the along track orbit configuration in which the differential solar radiation pressure and/or the differential atmospheric drag are acting on one plate to attempt to collapse the structure.



**Figure 13: Electrostatic Inflation of a test sandwich structure, from 0 kV to 9 kV**

The structure used in the test shown in Figure 13 consists of two 12x15 cm plates of 75 gauge aluminized Mylar. Three ribs of the aluminized Mylar connect the two plates. Charge was applied to the conducting sphere on which

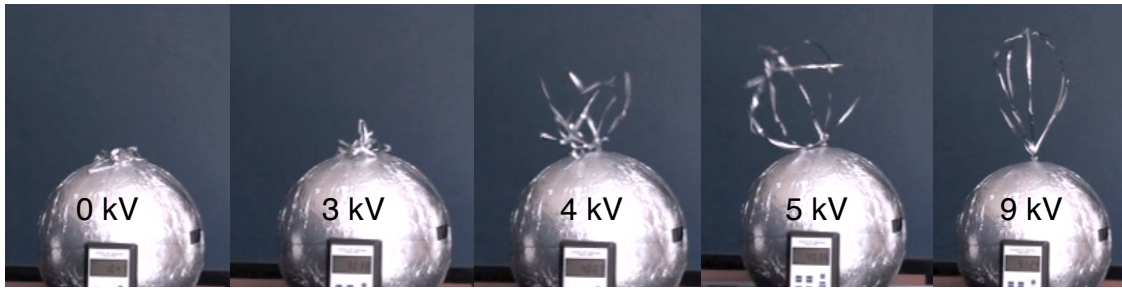


**Figure 14: Electrostatic Inflation of gossamer ribbon test structure, from 0 kV to 9 kV**

the sandwich structure rested. In the sandwich structure inflation experiment, inflation occurred between 7 and 13 kV. Figure 13 shows snapshots of the charging experiment. The duration of the inflation shown between the first and last frames of Figure 13 is approximately 5 seconds. This experiment clearly shows how a collapsed sandwich membrane structure can be inflated with kilo-Volt levels of potential. It should be noted here that the rib structures were simply glued to the outer membrane plates. This results in some bending stiffness of the ribs that is not accounted for in the earlier models. Despite these challenges, the experiments indicate that such self-supporting membrane structures can repeatedly and reliably be electrostatically inflated in a laboratory environment. Higher fidelity modeling of such lightweight structures is very challenging due to the strong nonlinear coupling between charge distribution and membrane shape. Adding the plasma space environment complicates the matter even further. Such experimental results are critical to explore experimentally appropriate material properties, construction methods, packing methods, and charging behaviors that lead to desirable membrane motions. Further, such testing will be used for validation and verification purposes of to be developed higher fidelity modeling of charged membrane structures.

Figure 14 shows the inflation of a gossamer ribbon structure, an example of a structure with large open surface segments. This ribbon structure was initially compacted to a height of approximately 2 cm, then inflated to a height of 25 cm. This experiment shows the potential of high deployed to stowed volume ratios with the electrostatic inflation concept. Notice in this photo series that the structure has obtained the fully inflated shape at 5 kV, yet gravity is preventing the structure from standing upright. As the voltage increases to 9 kV, the electrostatic repulsion between the ribbon structure and the conducting surface to which it is attached causes the entire structure to become upright as well as inflated to the desired shape.

Considering effects such as membrane wrinkling and stiffness in the ribs will be important when analytically modeling inflation in future work. The glue used to construct the structure also contributes to additional stiffness. It is expected that the actual inflation voltage would be larger than can be predicted analytically.

The relatively small potential levels required to inflate the sandwich structure in 1-g are promising to the concept of electrostatic inflation for space structures. As the orbital disturbance pressures are orders of magnitude smaller than the pressure due to gravity in the 1-g environment, required potential will be much smaller than required in lab experiments. It is even possible that natural charging phenomena in orbit will provide sufficient potentials for inflating gossamer structures. However, note that this paper has focused on the minimum required charge densities to overcome differential perturbations. In practice, the Gossamer structure should be inflated to much larger values to provide increased resistance to deformations.

## VII. Conclusion

This paper discussed the concept of using electrostatic forces for actuation of space structures consisting of lightweight membranes. A simple gossamer sandwich structure is used as the baseline structure for the study. The minimum required electrostatic forces required to maintain a nominal shape and offset disturbing orbital forces, such as differential gravity, drag and solar radiation pressure, are examined for three different orbit configurations. In contrast to the Coulomb research results on free-flying charged spacecraft, the differential solar radiation pressure is determined to be the dominant compressive disturbance force that must be compensated for. This force is orders of magnitude larger than differential gravity due to the very small Gossamer structure thickness and low mass of the membrane plates. Further, the study shows that the differential solar pressure will dominate for LEO altitudes larger than about 550 km. Below this the differential atmospheric pressures must be considered.

Laboratory experiments show that electrostatic inflation is feasible even in a 1-g environment. The pressure countering inflation is much larger in this 1-g environment, therefore potentials to inflate a structure in space could be

significantly lower than the 10 kV levels required in the lab. These potential levels are very feasible in space, as previous space experiments have achieved charging to this potential in both LEO and GEO. Much future work remains to explore and further understand this novel concept, but preliminary research shows promise for application of electrostatic inflation.

## Acknowledgments

The author would like to acknowledge Ira Katz for his help concerning the partially plasma shielded electrostatic force of a charged spherical body in a space environment.

## References

- <sup>1</sup>Freeland, R. E., Bilyeu, G. D., Veal, G. R., and Mikulas, M. M., "Inflatable Deployable Space Structures Technology Summary," *49th International Astronautical Congress*, Melbourne, Australia, Sept. 28 – Oct. 2 1998.
- <sup>2</sup>Freeland, R. E., Bilyeu, G. D., Veal, G. R., Steiner, M. D., and Carson, D. E., "Large Inflatable Deployable Antenna Flight Experiment Results," *Acta Astronautica*, Vol. 41, No. 4–10, 1997, pp. 267–277.
- <sup>3</sup>Banik, J. A. and Murphy, T. W., "Synchronous Deployed Solar Sail Subsystem Design Concept," No. AIAA-2007-1837, 47th AIAA Structures, Dynamics, and Mechanics of Materials Conference, 2007.
- <sup>4</sup>Cadogan, D. P., Lin, J. K., and Grahne, M. S., "Inflatable Solar Array Technology," No. AIAA-99-1075, 37th AIAA Aerospace Sciences Meeting and Exhibit, 1999.
- <sup>5</sup>Cadogan, D. P., Stein, J., and Grahne, M. S., "Inflatable Composite Habitat Structures for Lunar and Mars Exploration," *Acta Astronautica*, Vol. 44, 1999, pp. 399–406.
- <sup>6</sup>Jenkins, C. H. M., editor, *Gossamer Spacecraft: Membrane and Inflatable Structures Technology for Space Applications*, Vol. 191 of *Progress in Astronautics and Aeronautics*, American Institute of Aeronautics and Astronautics, 2001.
- <sup>7</sup>Cover, J. H., Knauer, W., and Maurer, H. A., "Lightweight Reflecting Structures Utilizing Electrostatic Inflation," US Patent 3,546,706, October 1966.
- <sup>8</sup>MacEwen, H. A., editor, *Stretched Membrane with Electrostatic Curvature (SMEC) Mirrors*, Vol. 4849. SPIE, December 2002.
- <sup>9</sup>King, L. B., Parker, G. G., Deshmukh, S., and Chong, J.-H., "Spacecraft Formation-Flying using Inter-Vehicle Coulomb Forces," Tech. rep., NASA/NIAC, January 2002.
- <sup>10</sup>Schaub, H., Parker, G. G., and King, L. B., "Challenges and Prospect of Coulomb Formations," *Journal of the Astronautical Sciences*, Vol. 52, No. 1–2, Jan.–June 2004, pp. 169–193.
- <sup>11</sup>Berryman, J. and Schaub, H., "Analytical Charge Analysis for 2- and 3-Craft Coulomb Formations," *AIAA Journal of Guidance, Control, and Dynamics*, Vol. 30, No. 6, Nov.–Dec. 2007, pp. 1701–1710.
- <sup>12</sup>Schaub, H., Hall, C., and Berryman, J., "Necessary Conditions for Circularly-Restricted Static Coulomb Formations," *Journal of the Astronautical Sciences*, Vol. 54, No. 3–4, July–Dec. 2006, pp. 525–541.
- <sup>13</sup>Natarajan, A. and Schaub, H., "Linear Dynamics and Stability Analysis of a Coulomb Tether Formation," *AIAA Journal of Guidance, Control, and Dynamics*, Vol. 29, No. 4, July–Aug. 2006, pp. 831–839.
- <sup>14</sup>Wang, S. and Schaub, H., "Switched Lyapunov Function Based Coulomb Control of a Triangular 3-Vehicle Cluster," *AAS/AIAA Astrodynamics Specialist Conference*, Pittsburgh, PA, Aug. 9–13 2009.
- <sup>15</sup>Seubert, C. R. and Schaub, H., "Tethered Coulomb Structures: Prospects and Challenges," *AAS F. Landis Markley Astrodynamics Symposium*, Cambridge, MA, June 30 – July 2 2008, Paper AAS 08–269.
- <sup>16</sup>McPherson, D. A., Cauffman, D. P., and Schober, W., "Spacecraft Charging at High Altitudes - The SCATHA Satellite Program," *AIAA Aerospace Sciences Meeting*, Pasadena, CA, Jan. 20–22 1975.
- <sup>17</sup>Mullen, E. G., Gussenhoven, M. S., Hardy, D. A., Aggson, T. A., and Ledley, B. G., "SCATHA Survey of High-Voltage Spacecraft Charging in Sunlight," *Journal of the Geophysical Sciences*, Vol. 91, No. A2, 1986, pp. 1474–1490.
- <sup>18</sup>Olsen, R. C., "Record Charging Events from Applied Technology Satellite 6," *J. Spacecraft*, Vol. 24, No. 4, 1986, pp. 362–366.
- <sup>19</sup>Katz, I., "Structure of the Bipolar Plasma Sheath Generated by SPEAR I," *Journal of Geophysical Research*, Vol. 94, No. A2, Feb. 1989, pp. 1450–1458.
- <sup>20</sup>King, L. B., Parker, G. G., Deshmukh, S., and Chong, J.-H., "Study of Interspacecraft Coulomb Forces and Implications for Formation Flying," *AIAA Journal of Propulsion and Power*, Vol. 19, No. 3, May–June 2003, pp. 497–505.
- <sup>21</sup>Hobbie, R., *Intermediate Physics for Medicine and Biology*, Springer, 3rd ed., 1997.
- <sup>22</sup>Ansoft, *User's Guide: Maxwell 3D*, 11th ed., Jan. 2010.
- <sup>23</sup>Bittencourt, J. A., *Fundamentals of Plasma Physics*, Springer, 3rd ed., 2004.
- <sup>24</sup>Hastings, D. E. and Garrett, H. B., *Spacecraft-Environment Interactions*, Cambridge University Press, 1996.
- <sup>25</sup>Pierrard, V., Goldstein, J., André, N., Jordanova, V., Kotova, G., Lemaire, J., Liemohn, M., and Matsui, H., "Recent Progress in Physics-Based Models of the Plasmasphere," *Space Science Reviews*, Vol. 145, No. 1, 05 2009, pp. 193–229.
- <sup>26</sup>Garrett, H. B. and DeForest, S. E., "An Analytical Simulation of the Geosynchronous Plasma Environment," *Planetary Space Science*, Vol. 27, 1979, pp. 1101–1109.
- <sup>27</sup>Lennartsson, W. and Reasoner, D. L., "Low-Energy Plasma Observations at Synchronous Orbit," *Journal of Geophysical Research*, Vol. 83, No. A5, 1978, pp. 2145–2156.
- <sup>28</sup>Thiebault, B., Hilgers, A., Sasot, E., Laakso, H., Escoubet, P., Génot, V., and Forest, J., "Potential Barrier in the Electrostatic Sheath around a Magnetospheric Spacecraft," *Journal of Geophysical Research*, Vol. 109, No. A12207, 2004.
- <sup>29</sup>Murdoch, N., Izzo, D., Bombardelli, C., Carnelli, I., Hilgers, A., and Rodgers, D., "Electrostatic Tractor for Near Earth Object Deflection," *59th International Astronautical Congress*, Glasgow, Scotland, 2008, Paper IAC-08-A3.1.5.

<sup>30</sup>Vallado, D. A., *Fundamentals of Astrodynamics and Applications*, Space Technology Library, Springer, 3rd ed., 2007.